Water Research 158 (2019) 171–181

Contents lists available at ScienceDirect

Water Research

journal homepage: www.elsevier.com/locate/watres

Effects of copper ions on removal of nutrients from swine wastewater and on release of dissolved organic matter in duckweed systems

Qi Zhou [a, b, c, 1], Xiang Li [b, 1], Yan Lin [b, 1], Chunping Yang [a, b, c, d, *], Wenchang Tang [b], Shaohua Wu [b], Dehao Li [a, c, **], Wei Lou [d]

[a] School of Environmental Science and Engineering, Guangdong University of Petrochemical Technology, Maoming, Guangdong, 525000, China
[b] College of Environmental Science and Engineering, Hunan University and Key Laboratory of Environmental Biology and Pollution Control (Hunan University), Ministry of Education, Changsha, Hunan, 410082, China
[c] Guangdong Provincial Key Laboratory of Petrochemcial Pollution Processes and Control, Guangdong University of Petrochemical Technology, Maoming, Guangdong, 525000, China
[d] Hunan Province Environmental Protection Engineering Center for Organic Pollution Control of Urban Water and Wastewater, Changsha, Hunan, 410001, China

ARTICLE INFO

Article history:
Received 8 March 2019
Accepted 15 April 2019
Available online 19 April 2019

Keywords:
Copper
Dissolved organic matter
Duckweed
Nutrient
Swine wastewater

ABSTRACT

High concentration of Cu^{2+} in swine wastewater raises concerns about its potential adverse effects on nutrient removal by aquatic plants like duckweed. In this work, the effects of copper ions on nutrient removal and release of dissolved organic matter (DOM) were investigated in duckweed systems. Results showed that the removal performance of ammonia nitrogen (NH_3–N) and total phosphorus (TP) increased at 0.1–1.0 mg/L of Cu^{2+}, while dropped at 2.0–5.0 mg/L of Cu^{2+}. A novel kinetic model in which Cu^{2+} was taken into account was then developed which was used to optimize Cu^{2+} concentration at 0.96 mg/L for nutrient removal in duckweed systems. NADH, detected in DOM by the parallel factor (PARAFAC) analysis, exhibited high capacities of binding copper ions, so it played an important role on the decrease of Cu^{2+} concentrations in duckweed systems. The principle component analysis (PCA) showed that the dominant DOM were lower molecular weight compounds at 1.0 mg/L of Cu^{2+} and higher molecular weight compounds at 2.0–5.0 mg/L of Cu^{2+}. The bonds of C–H (humic-like), N=O (NO_3^-) and Ar–H (tyrosine) in DOM were responsible for not only the fastest binding with Cu^{2+} from the result of the two-dimensional Fourier transform infrared correlation spectroscopy (2D-FTIR-CoS) but also the variations of DOM conformations at a critical concentration of 0.5 mg/L Cu^{2+} from the perturbation correlation moving window two-dimensional (PCMW2D) analysis. These findings lead to a better understanding on the environmental behaviors and mechanisms of Cu^{2+} in duckweed systems.

1. Introduction

Heavy metals including copper and zinc in swine wastewater have been paid close attention due to their potential to inhibit the growth of various aquatic plants and microorganisms (Du et al., 2018; Tandon et al., 2013), and pose severe challenges to traditional treatment processes including microbiological treatment and phytoremediation for swine wastewater. Therefore, various methods and processes have been proposed and been reported to address this pollution (Wang and Chen, 2009; Wen et al., 2016). Duckweed used in phytoremediation for swine wastewater treatment has shown high potential for removing nutrients, maximizing biomass yield and easily harvesting (Cheng and Stomp, 2009; Li et al., 2017). It was reported that the major pathways for nutrient removal were through duckweed uptake and nitrification/denitrification by bacteria in a duckweed pond (Luo et al., 2016; Pant and Adholeya, 2009; Xu and Shen, 2011). Although trace of certain heavy metals such as copper is essential for living cell functions, it would be deleterious to many organisms via the destruction of anti-oxidative defense system when its

* Corresponding author. School of Environmental Science and Engineering, Guangdong University of Petrochemical Technology, Maoming, Guangdong, 525000, China
** Corresponding author. School of Environmental Science and Engineering, Guangdong University of Petrochemical Technology, Maoming, Guangdong, 525000, China.
E-mail addresses: yangc@hnu.edu.cn (C. Yang), dehlee@163.com (D. Li).
[1] These authors contribute equally to this paper.

https://doi.org/10.1016/j.watres.2019.04.036
0043-1354/

concentration is high (Chen et al., 2015a; Obermeier et al., 2015; Wu et al., 2017). Consequently, high metal loads could inhibit the duckweed growth, thereby reduce the capacity of nutrient removal by duckweed and even cause the complete failure of nutrient removal in phytoremediation (Li et al., 2018). For instance, the removal rate of NH_3—N decreased from 85% to 25% when the Zn^{2+} concentration increased from 0 to 15 mg/L in swine wastewater (Zhou et al., 2018).

Several mathematic models were developed to take into account of the influence of heavy metals on nutrient removal from wastewater treatment, which include the first-order model (Vermaat and Hanif, 1998), Michaelis-Menten model (Vermaat and Hanif, 1998), and Logistic model (Zhang et al., 2014). In these models, the removal rate represented the comprehensive effects of a series of biotic and abiotic factors such as temperature, photoperiod and phosphorus-nitrogen concentrations (Chen et al., 2018; Cheng et al., 2016). However, these models are still not sufficient because they can only indirectly reflect the real effect of heavy metals via the decrease or increase of removal rate (Yang et al., 2018; Zhang et al., 2014). To our knowledge, few kinetic models incorporating the concentration of heavy metals were available for the description of the influence of heavy metals on duckweed systems. Thus, more investigations are needed to develop better mathematical models in which heavy metal concentration can be taken into account.

To alleviate the stress of heavy metals on nutrient uptake, aquatic plants can produce various antioxidants through the antioxidative defense system (Cakmak, 2010). Dissolved organic matter (DOM), naturally occurring antioxidant, is a heterogeneous mixture derived from metabolic excretion or autolysis of cells in aquatic plants and rhizosphere microorganisms (Senga et al., 2018). DOM fractions may contain labile low molecular weight (LMW) substances and more stable high molecular weight (HMW) substances (Rengel, 2002). LMW materials refer to carbohydrates, small proteins/peptides, organic acids (OA), amino acids, vitamins, hormones, etc (Rengel, 2002). HMW compounds mainly contain humics, mucilage polysaccharides, secretory proteins and ectoenzymes (Matthias et al., 2007). So, there are abundant organic functional groups (e.g., amide, carboxyl, phenol, and hydroxyl) with high active sites in DOM. And these functional groups can efficiently combine heavy metals via chelation or complexation (Peng et al., 2018). For example, LMW-OA concentration in root exudates was positively correlated with the amount of Cd accumulated in millet roots (Chiang et al., 2011). It implied that DOM could reduce the concentration of heavy metals, so the toxicity of heavy metals to aquatic systems could be relieved. However, the interaction mechanisms between DOM and heavy metals are still not clear in duckweed systems.

The interactions of heavy metal ions with DOM can be revealed as the change on composition and structure of DOM. The composition of DOM could be detected by the fluorescence excitation-emission matrix (EEM) spectroscopy combined with parallel factor (PARAFAC) analysis, which can reduce the interferences due to overlapping fluorophores among various compounds and determine the individual fluorescent components in DOM (Yamashita and Jaffe, 2008). However, the effect of the interactions between heavy metals and DOM on change of fluorescent components remains unclear, for example, the relation between each fluorescent component and each heavy metal concentration (Yamashita and Jaffe, 2008). Principal components analysis (PCA) has become an efficient statistical tool on the identification of differences and similarities between components and external factors in a data set by analyzing the loading plots and score plots (Abdulla et al., 2013). In activated sludge process, the joint application of PCA and EEM-PARAFAC can provide overall assessment on the modifications of dissolved organic nitrogen (DON) components at different solids retention time (Hu et al., 2018). While the joint application of PCA and EEM-PARAFAC used in duckweed systems has not been reported.

In addition, the variation of the molecular structure in DOM also needs further investigation. Fortunately, the two dimensional Fourier transform infrared correlation spectroscopy (2D-FTIR-CoS) has the potential to provide a comprehensive insight into the features of functional groups on DOM which included fluorescent and non-fluorescent components under the heavy metal perturbation (Lumsdon and Fraser, 2005). The binding sites and binding orders of DOM to heavy metals can be probed by the synchronous and asynchronous spectra of 2D-FTIR-CoS (Abdulla et al., 2010). Furtherly, perturbation correlation moving window two-dimensional (PCMW2D), proposed recently based on 2D-FTIR-CoS, has become a powerful tool to explore the conformational variation of DOM with perturbation (e.g., temperature, concentration, etc.) (Morita et al., 2006). In PCMW2D analysis, the perturbation induced spectral transition points can be obtained from the correlation intensity along the perturbation variables' direction (Noda, 2014). However, few studies have been reported to use the above combined techniques to analyze the variation on composition and molecular structure of DOM affected by various concentrations of Cu^{2+}. Therefore, in depth examination on the mechanisms of the interactions between heavy metals and duckweed on nutrient removal and DOM release is necessary, which would provide valuable information on the optimum condition and maximum capacity of phytoremediation technology in swine wastewater contaminated by heavy metals and the microcosmic transport of heavy metals in natural and engineered environments.

In this work, we have developed a comprehensive mathematical kinetic model in which Cu^{2+} concentration was taking into account to describe the effect of Cu^{2+} on nutrient removal in duckweed systems for swine wastewater treatment. In addition, the joint application of EEM-PARAFAC, PCA, 2D-FTIR-CoS and PCMW2D was proposed to better understand the mechanisms of the interactions between DOM to copper ions at the molecular scale which include DOM compositions, binding sites, binding orders, and DOM conformations. The objective of this research is to elucidate the influence mechanisms of Cu^{2+} on nutrient removal by duckweed via the novel kinetic model, and explore Cu-DOM interactions by using the 3D fluorescence maps and 2D-FTIR-CoS technologies in duckweed systems. It is expected to lead to a better understanding of the transport and fate of Cu and providing an improved approach to design and manage duckweed systems for the treatment of swine wastewater contaminated by heavy metals.

2. Materials and methods

2.1. Experimental procedure

The initial media was prepared as synthetic swine wastewater and its ionic concentrations were listed in Table S1 for the batch tests according to our previous works. Different volumes CuSO4•5H2O solution was added into the initial media to simulate different Cu^{2+} concentrations (0.1, 0.5, 1.0, 2.0, and 5.0 mg/L). And the initial synthetic wastewater did not have a fluorescence signature through the measurement of fluorescence EEM (Fig. S6). The pH value of media was adjusted at 6.30 ± 0.40 by using 0.10 mol/L HCl solution. Then, the initial media was sterilized in an autoclave for 30 min at 121 °C before duckweed was added into the media. Eighty-four beakers (500 mL, 6.4 cm × 6.4 cm × 12.5 cm) including 2×7 control beakers without extra copper ions and $2 \times 5 \times 7$ duplicate sample beakers with extra copper ions were used in five batch tests. Each beaker contained 140 mL (3.4 cm deep

in the beaker) of media, and it was initially seeded with the same amount (0.4 ± 0.1 g fresh weight) of duckweed to cover the 80% surface area of 6.4 cm × 6.4 cm.

Prior to culture initiation, the duckweed had been pre-cultured in our previous works (Zhou et al., 2018). And then the healthy duckweed was selected and cleaned by distilled water. All beakers were placed into a light growth chamber with 16 h photoperiod at 25 °C and a photosynthetic photon flux density of 70 ± 10 μmol m^{-2} s^{-1} provided by wide spectrum fluorescent tubes. Due to the decrease of pH as the duckweed grew, 0.10 mol/L NaOH solution was added to maintain the pH around 6.30 ± 0.40. Destructive sampling was used to monitor the nutrient level, DOM concentrations and duckweed growth by taking a whole beaker as a sample for analysis. Duplicate samples and control samples were collected and analyzed every 4–8 days for 38 days.

2.2. Spectral determination and analysis

In this study, DOM was designated as dissolved organic carbon (DOC) passing through a 0.45 μm membrane filter. Its concentration was measured by a Shimadzu TOC-VCPH analyzer (Shimadzu, Japan) (Fig. S5). Before the measurement of EEM spectra, the DOC concentrations of all of the samples were diluted <10 mg/L, and thereby the samples have an absorbance at λ = 254 nm (Abs_{254}) < 0.2 to minimize inner filter effects during fluorescence analysis (Poulin et al., 2014) (see details in the Supporting Information, Fig. S7). DOM fluorescent components were analyzed by 3D fluorescence maps which were measured by using a F-4600 fluorescence spectrophotometer equipped with a 150W xenon lamp (Hitachi, Japan). Scanning emission (Em) spectra from 200 to 600 nm were obtained in 2 nm increments by varying the excitation (Ex) wavelength from 200 to 500 nm in 10 nm increments at room temperature. The EEM spectra were recorded at a scan rate of 12000 nm/min, and the slit widths of both the excitation and emission were set as 10 nm. And the PARAFAC analysis was presented in the Supporting Information.

For collecting Fourier transform infrared spectroscopy (FTIR) analysis, the solid-state DOM was extracted by a freeze drier (Biobase, China) from water samples. And then the mixtures of 1.0 mg freeze-dried DOM sample and 100 mg potassium bromide (KBr, IR grade) were ground and homogenized to reduce light scatter, and then compressed to form a disk under 15 MPa for 2 min. Finally, the disk were measured to obtain FTIR spectra by using an IR Affinity-1 spectrometer (Shimadzu, Japan) at a resolution of 4 cm^{-1} with 20 scans over 4000-400 cm^{-1} at room temperature. And the Two-dimensional correlation analysis was presented in the Supporting Information.

2.3. Wastewater analysis

Duckweed was harvested from each beaker by using a strainer with 0.5 mm pore size. Then, the fresh weight of duckweed was measured using a balance immediately after the duckweed harvested was placed on paper towels for 5 min (Fig. S2). After duckweed harvested, the wastewater were analyzed for NH_3–N, TP, Cu. NH_3–N was determined by the Nessler's reagent colorimetric method, and TP was used in the potassium persulfate digestion colorimetric method according to the standard methods (EPA of China, 2002). The Cu^{2+} concentration was measured by an atomic absorption spectrometer (AAS, Agilent 3510, USA).

2.4. Statistical analysis

The results calculated were expressed as mean ± SE (standard error) of three replicates in water and duckweed samples for each treatment. One-way ANOVA was performed to compare all data. Statistical analyses were conducted using SPSS 17.0 (SPSS, Chicago, IL, USA), with significance level $p < 0.05$. Obtained models followed by Tukey's HSD tests were used to identify any significant differences between treatments. PCA was performed by using the PAleontological STatistics software (PAST, version 3.0), which based on the data of the maximum fluorescence intensity from PARAFAC results.

3. Results and discussion

3.1. Performance of nutrient removal by duckweed at various Cu^{2+} concentrations

In this study, removal curves of nutrients were fitted by using First-order kinetic model, Michaelis-Menten kinetic model and Modified logistic kinetic model (see details in the Supporting Information). The important parameters of fitting results for the ammonia nitrogen (NH_3–N) and total phosphorus (TP) removal by the three models under different Cu^{2+} concentrations were integrated in Table S2. The Modified logistic kinetic model had a higher R^2 value than that of other two models at each concentration of Cu^{2+}. It was suggested that Modified logistic kinetic model could describe better the nutrient removal by duckweed exposed to various Cu^{2+} concentration levels. And the fitting plots were showed in Fig. 1 and Fig. S1. As seen in Fig. 1, judging from the results of the control groups, the removal rate of NH_3–N and TP were 85% and 99%, respectively when the test came to the end. It suggested that duckweed had a good removal rate of NH_3–N and TP from ADSW that was not contaminated by Cu^{2+}, which was in agreement with the results of our previous study (Zhou et al., 2018).

Besides, the performance of nutrient removal also exhibited different trends at various Cu^{2+} Concentrations. As seen in Fig. 1 and Table S2a, compared with the control (0 mg/L Cu^{2+}), the removal rate (r_m) of NH_3–N and TP was larger at 0.1–1.0 mg/L Cu^{2+}, while that was lower at 2.0–5.0 Cu^{2+} mg/L. Interestingly, the removal performance of NH_3–N could be improved at lower Cu^{2+} concentrations but that was inhibited at higher Cu^{2+} concentrations. This phenomenon can be explained by the fact that excess Cu^{2+} (>2.0 mg/L) would do harm to direct assimilation of duckweed and biodegradation of rhizosphere microorganisms, which were two major pathways for nutrient removal by duckweed (Cheng et al., 2002; Xu and Shen, 2011). For instance, high Cu^{2+} concentrations could result in the disintegration of antioxidant systems by producing a large amount of reactive oxygen species (ROS) in duckweed cells (Wu et al., 2018) and cause the inhibition activity such as the nitrification-denitrification in rhizosphere microorganisms (Obermeier et al., 2015).

On the contrary, low Cu^{2+} concentrations could be beneficial to the removal of NH_3–N. This was in good agreement with findings by Obermeier et al. (2015), who found the decrease of peroxidase activity (POX) in low Cu^{2+} concentrations. The low Cu^{2+} dosage may reduce the eutrophic stress from high initial concentrations of NH_3–N and TP on duckweed through stimulating the ROS scavenging systems to function (Asada, 1987). Similar trends were observed on the removal of TP by fitting Modified logistic kinetic model (Table S2b). Therefore, further work was needed to elucidate the relation between eutrophic stress and Cu^{2+} stress and find out the real inflection point of Cu^{2+} concentration.

3.2. Modeling of nutrient removal under different Cu^{2+} concentrations

In the Modified logistic kinetic model, the parameter Q represents external environmental stress, and there mainly exists

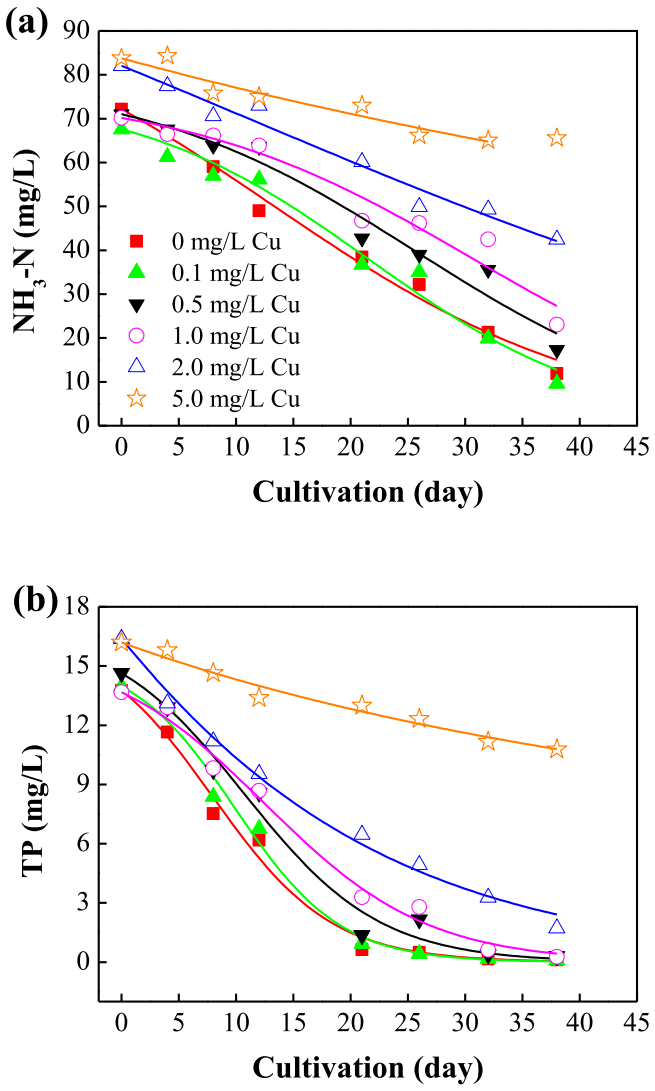

Fig. 1. Modified logistic model for Nutrient removal by duckweed under various Cu^{2+} concentrations within 38 days. (a) NH_3–N; (b) TP.

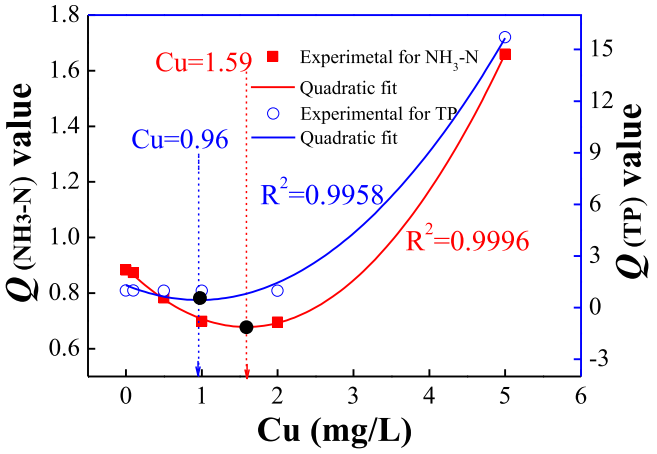

Fig. 2. Quadratic fit of relationship between Cu^{2+} concentrations and Q value.

external pressure caused by Cu^{2+} in duckweed systems. It meant that the relation between Q value and Cu^{2+} concentration may be described by a mathematical formula, and thereby the scatter diagram was plotted by Cu^{2+} concentrations on the horizontal axis and Q values on the vertical. As shown interestingly in Fig. 2, the connected curve by point was close to the quadratic curve. So, the curves were fitted iteratively by least squares method, and then the equations were obtained by:

$$Q_N = 0.0843 \times Cu^2 - 0.2678 \times Cu + 0.8905 \quad (1)$$

$$Q_P = 0.9327 \times Cu^2 - 1.7931 \times Cu + 1.3059 \quad (2)$$

Here, the correlation coefficient (R^2) of equations (1) and (2) was 0.9996 and 0.9958, respectively, implying that equations (1) and (2) could commendably describe the relationship between the Cu^{2+} concentration and Q value. It meant that the external environmental stress could be adjusted by various Cu^{2+} concentrations. Moreover, it was found that the inflection point of Cu^{2+} concentration for removal of NH_3–N and TP were 0.96 mg/L and 1.57 mg/L, respectively (Fig. 2), which suggested that they can be applied for estimating the degree of environmental stress induced by copper ions in duckweed systems.

Apart from that, the inflection point of Cu^{2+} concentration on removal of total phosphorus (TP) was lower than on removal of ammonia nitrogen (NH_3–N), showing that removal of TP was more susceptive to Cu^{2+} concentration. It was concluded that the inhibiting effect on removal of TP at a given Cu^{2+} concentration was stronger than that on removal of NH_3–N by duckweed. This finding might be ascribed to the different removal mechanisms of NH_3–N and TP in a duckweed system. Duckweed uptake was the dominant pathway for TP removal, while ammonia volatilization and nitrification were also the major pathways except duckweed uptake in a duckweed pond (Xu and Shen, 2011).

Thus, according to the Liebigs law of minimum, the optimal Cu^{2+} concentrations might be chosen as 0.96 mg/L in order to minimize environmental pressure for better nutrient removal by duckweed. Moreover, the Modified logistic kinetic model could be simplified by equations (3) and (4):

$$\frac{dC_N}{dt} = -rC_N(0.0843Cu^2 - 0.2678Cu + 0.8905) \quad (3)$$

$$\frac{dC_P}{dt} = -rC_P(0.9327Cu^2 - 1.7931Cu + 1.3059) \quad (4)$$

As shown in equations (3) and (4), the novel kinetic model, named Cu-effect kinetic model, was clear because there were no complicated parameters. It was suggested that the Cu-effect kinetic model could contribute to adjust the actual removal rate of duckweed by modifying Cu^{2+} concentration in duckweed systems. Although the novel kinetic model was limited to the hypothesis that there was only the eutrophic stress and copper stress in duckweed systems, it creatively introduced the Cu^{2+} concentrations into the kinetic model to describe the effect of Cu^{2+} on nutrient removal in duckweed systems for swine wastewater treatment. It was meaningful to provide a tool for the quantification of the influence caused by heavy metals on phytoremediation processes and to advance modeling of nutrient removal in biogeochemical cycling of aquatic ecosystems.

3.3. DOM characterization analyzed by using EEM-PARAFAC

The EEM spectra of samples at different Cu^{2+} concentrations were analyzed by PARAFAC. The results revealed that the appropriate number of components was four based on the results of split half analysis as well as residuals and loadings analysis (Fig. 3). Additionally, to further clarify fluorescence DOM spectra, the

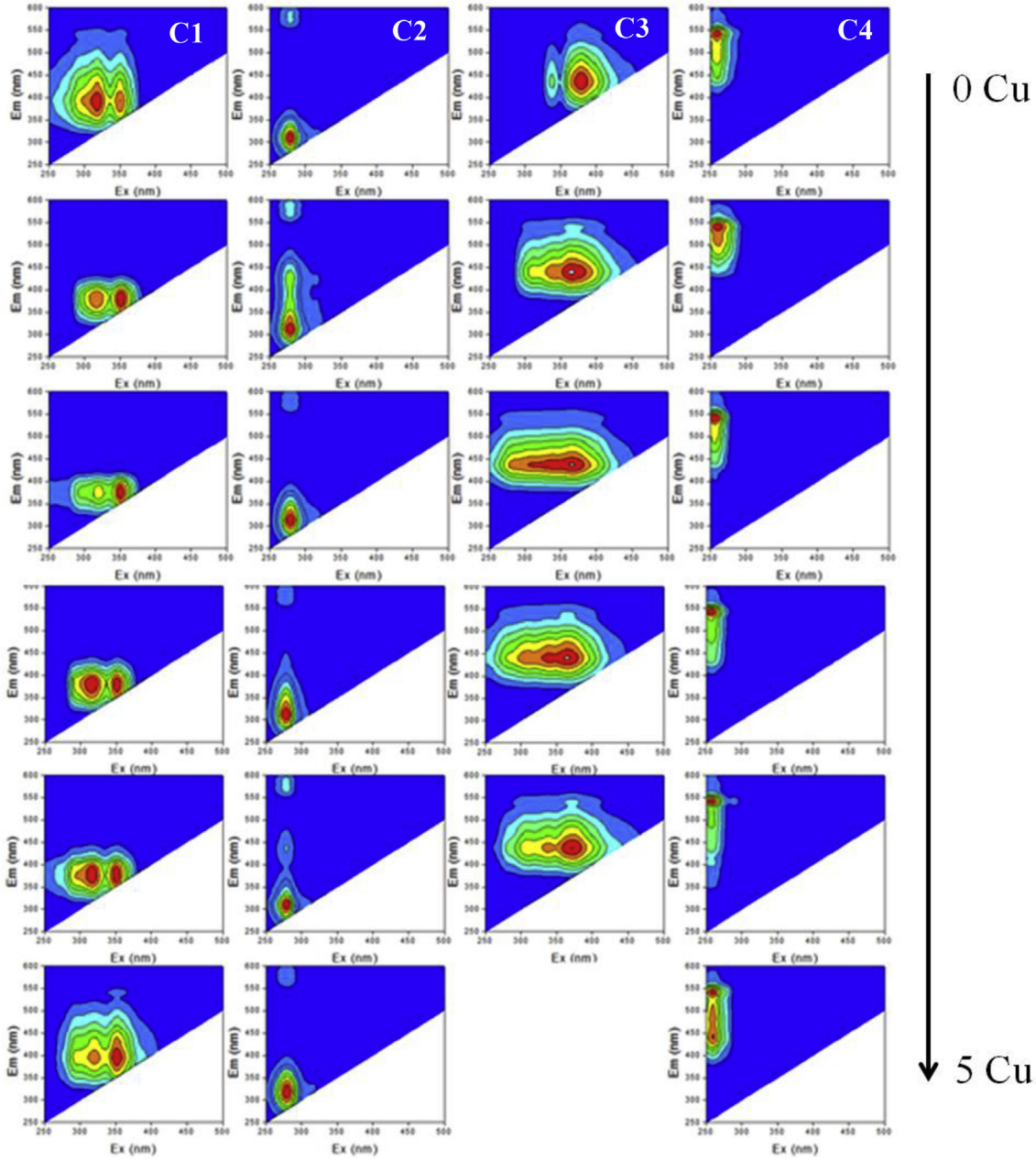

Fig. 3. EEMs of the four components derived from PARAFAC analysis under various Cu^{2+} concentrations in the duckweed systems.

additional experiment with duckweed at various Cu^{2+} concentrations, which repeated previous batch experiments except the destructive sampling and sampling interval, has been performed within 15-days culture time (see details in the Supporting Information). And the EEM spectra of additional experiment were presented in Fig. S8. As shown in Fig. S8, it can be demonstrated that there actually were four components in the DOM released from the duckweed system. Thus, combining with Fig. 3 and Fig. S8, the positions of peaks should have a broad range for better understanding. And the positions of peaks of these four components have been illustrated in Table 1.

As summarized in Table 1, four components identified by the PARAFAC model, including one microbial humic-like substances (C1), one tyrosine-like substance (C2), NADH (C3) and humic-like substances (C4). C1 (Ex/Em = 280–350/370), which was similar to microbial humic-like found by Murphy et al. (2011), was considered to be produced and altered by microbial reprocessing from the biodegradation of the leaves and roots (Wei et al., 2009). C2 (Ex/Em = 270–280/310-320), which resembled tyrosine-like substance found by Zhu et al. (2017), belonged to the type of protein-like materials and was also observed in other aquatic environments (Kowalczuk et al., 2009). Additionally, C2 missed the 220–240 nm excitation peaks comparing with typical peak of tyrosine-like. One explanation was the effect of "shadow components" induced by the interactions with metal ions and higher sensitivity of tyrosine-like (Murphy et al., 2011). C3 (Ex/Em = 340–370/440-450), which was related to NADH (Arunachalam et al., 2005; Li et al., 2008, 2011; Teixeira et al., 2011). The NADH, a kind of coenzymes existed in all living cells, are the major intermediate electron and hydrogen carriers that couple the substrate catabolism with respiration and

Table 1
Description of the identified EEM-PARAFAC components.

components	Ex/Em maxima (nm)	description	references
C1	280-350/370	microbial humic-like substance	Murphy et al. (2011); Wei et al. (2009)
C2	270-280/310-320	Tyrosine-like substance	Kowalczuk et al. (2009); Zhu et al. (2017)
C3	340-370/440-450	NADH	Arunachalam et al. (2005); Li et al. (2008); Li et al. (2011); Teixeira et al. (2011)
C4	260/270, 420-540	humic-like sustance	Rosario-Ortiz et al. (2007); Zhu et al. (2014)

anabolism (Arunachalam et al., 2005). However, the fluorophores of C3 need further clarification by spiking experiments because other fluorophores, such as humic-like and fulvic-like fluorescence, will be also likely to fluoresce in this region. C4 (Ex/Em = 260/270, 420–540), which corresponded to humic-like substances found by Zhu et al. (2014). They stated a component with one excitation emission around 250–260 nm and two emission peaks centered around 250 nm and 500 nm, but that component was not identified. While according to the report of Rosario-Ortiz et al. (2007), peaks at excitation wavelengths (250–470 nm) and emission wavelengths (380–580 nm) were related to humic acid-like organics. Therefore, the component C4 was classified as humic-like substance. And because the peaks occurred in the boundary of forbidden regions (Em > 2Ex), Thus, it remains to be elucidated whether the peak in the boundary of the forbidden regions actually existed, or its existence is due to the different constraints or criteria imposed during modeling, or due to an interaction between each fluorescence component. More discussion on the peaks of C4 was illustrated in Supporting Information.

To further verify the fluorophore species of component C3, the spiking experiments with the water samples dosed with NADH was carried out (specific procedure of spiking experiment was seen in the Supporting Information). The fluorescence maps of component C3 in the water samples dosed with NADH at 0 Cu^{2+} concentrations were shown in Fig. S9b. The fluorescence peak locations were similar to those of Fig. S9a, while the corresponding fluorescence peak intensity was strengthened significantly, indicating that the dosed analytes were in accordance with the fluorophores in the water samples from duckweed system. It was demonstrated that the component C3 was NADH, which provided a strong evidence. In general, the NADH fluorescence would typically exhibit an immediate step increase when the system was switched from aerobic to anoxic/anaerobic conditions (Arunachalam et al., 2005). So the dissolved oxygen (DO) of duckweed system in the additional experiment was also monitored by using dissolved oxygen meter (JPB-607A, Qiwei Co., China) as the duckweed grew. The DO values of duckweed system in various culture times were presented in Fig. S10, which suggested that the DO values of duckweed system were unstable, and the duckweed system experienced the aerobic process and anoxic process conditions (DO = 1–3 mg/L) as duckweed grown on the water surface. Thus, the NADH could be accumulated and detected under the aerobic and anoxic condition, which provided another evidence for that the component C3 was NADH.

Probably, other fluorophores compounds such as typical humic-like and fulvic-like substances could emit fluorescence in the broad region (Ex/Em = 370/440 nm), while this observation usually occurred in the stable aerobic process (Li et al., 2011). Therefore, it was confirmed that the main peaks of this broad region belonged to the NADH, and other inert products in this region such as humic or fulvic acids like substances were so weak that they might be concealed in the fluorescence of NADH due to the aerobic and anoxic conditions.

Additionally, the excitation and emission characteristics of traditional peaks and their description were displayed in Table S3. Compared with the location of traditional peaks, components (C1, C2, C3 and C4) appeared to have unusual fluorescence spectra, and their positions shifted towards the longer wavelengths (red-shifted) or the shorter wavelengths (blue-shifted). Besides, the environment of the fluorophore, such as temperature, solvent, hydrogen-bonding, pH, metal ions and the presence of other solutes can also influence the positions of peaks (red-shifted or blue-shifted) (Senesi, 1990). So, to verify the effect of these factors on the position and shape of peaks, the pH-spiking experiment and metal-spiking experiment were also carried out (Figure S11, S12 and S13), which confirmed that the high concentrations of proton and copper ions as well as the presence of other components could cause the variation of fluorescence spectra (see detail in the Supporting Information). On the whole, the shifts towards longer or shorter wavelengths in this study, which exhibited unusual fluorescence spectra, were acceptable to reflect the characteristics of duckweed system. However, due to the complexity of duckweed system, the combined effect caused by pH, copper ions and other component in DOM remained to be elucidated in duckweed system. Clearly, PARAFAC spectra from DOM data sets describe the probabilistic distribution of an ensemble of individual spectra belonging to a range of spectrally similar chemical moieties from a range of sources, rather than the exact chemical spectra (Murphy et al., 2011). Therefore, many unidentified components and their impacts on water treatment process have not been investigated. In the treatment process by duckweed, to study the variations of unknown components and to create a classification of DOM fractions, which are contributive to the design and selection of duckweed systems.

3.4. *Effect of Cu^{2+} concentration on the fluorescent components of DOM*

The fluorescent components of DOM released from the duckweed systems at different Cu^{2+} concentrations were conducted by EEM-PARAFAC. PARAFAC modeling of these water samples produced four component models (C1–C4, Fig. 3) at various initial Cu^{2+} concentrations ranging from 0 to 4.0 mg/L, but there was only three component models (C1, C2 and C4) at initial Cu^{2+} concentration of 5.0 mg/L. It was indicated that C3 (NADH) was significantly influenced by Cu^{2+} concentrations. Generally, the NADH, a kind of intracellular fluorophores, was originated from the metabolism of anaerobic microorganisms during their growth and substrate degradation process (He et al., 2017; Li et al., 2011). The disappear of C3 at 5 mg/L Cu^{2+} could be explained that NADH was predicted to have high binding affinity for heavy metals due to the abundant carboxylic and phenolic groups which were generally considered as strong binding sites with copper ions in DOM. Additionally, with the concentration of Cu^{2+} increased, the more binding sites were occupied by copper ions, so the non-fluorescent chelate compound (Cu-NADH) was formed, and thereby the fluorescence of NADH disappeared at higher Cu^{2+} concentration (5 mg/L Cu^{2+}). On the other hand, the copper ions could also bond with NADH to develop a new electron transfer chain and promote the conversion of NADH to NAD^{+} which had no fluorescence at higher Cu^{2+} concentrations (Li et al., 2011; Sun et al., 2011).

Moreover, the quenching curves of each fluorescence

component at various Cu^{2+} concentrations were shown in Fig. S4. C3 component (NADH) also showed an obvious fluorescence quenching with exhibiting a clear downward trend, while other components (C1, C2 and C4) showed larger fluctuations with the increase of Cu^{2+} concentrations, indicating that NADH played a vital role on the binding of DOM to heavy metals. The key components distributed within various fractions of DOM were the main influence on the impact of metal binding. Recognizing the different roles of various components played in heavy metal binding, several strategies could be adopted for risk control of heavy metal migration (Wu et al., 2012). For instance, treatment processes with high ratios of NADH, should be encouraged.

In addition, larger fluctuations in the quenching curves were also observed in a study conducted by Yamashita and Jaffe (2008), who employed PARAFAC-EEM quenching to explore the interactions between surface water-borne DOM and Cu. Yamashita and Jaffe (2008) found that protein-like components increased slightly with the initial addition of Cu and then decreased with increasing the initial Cu additions. There were three reasons for the increases in fluorescence intensity. Including 1) the changes in quantum yields of protein fluorescence by three-dimensional structural change of protein molecules might have occurred due to the high concentrations of Cu^{2+}. 2) The fluorescence intensity of such quenched protein-like components might be enhanced through the replacement of the original quencher with Cu^{2+}. 3) The fluorescence intensity might also be enhanced due to the replacement of the protein in the DOM-protein complexes through the interaction with Cu whereby the formation of more stable DOM-Cu complexes result in the release of protein-like components. Based on the above explanations, in the duckweed system, the larger fluctuations of C1, C2 and C4 component in quenching curves might be a result of the stable complexes in molecular environments of microbial humic-like, tyrosine –like and humic-like substances with metals. And, as shown in Fig. S3, the Cu^{2+} concentrations had a slight decrease as the cultivated time increased, which was likely to be caused by the combined effect of C1, C2, C3 and C4 component with copper ions. Often, interactions with DOM and metals are characterized by just one quenching constant which is an oversimplification of the complexation process (Ohno et al., 2008). In fact, the interactions between organic matter and metal were complex, which could exhibit not only quenching but also enhancement in fluorescence intensity. So, a non-monotonic change in quenching curves should be possible. Additionally, these results suggested that the method of fluorescence quenching may not be appropriate for the evaluation of the binding characteristics of C1, C2 and C4 components released from duckweed system and metal ions. Therefore, further studies are needed to clarify such changes in molecular environments of these components and assess their environmental significance. Therefore, in the next section of this paper, we combined principal components analysis (PCA) with EEM-PARAFAC to further identify and classify the behaviors of the four fluorescence components at various Cu^{2+} concentrations.

Furtherly, to determine the binding capability for NADH, the log K_M value was calculated by using the modified Stern–Volmer Model (see details in Supporting Information) which was widely applied in monotonic change of quenching curves. The stability constant (log K_M value) was 5.65, which was a relatively high value for Cu-DOM reported in lake sediment-derived and landfill leachate-derived (Wu et al., 2012; Xu et al., 2013). It was indicated that NADH in DOM exhibited high capacities of binding copper ions and was also an important metal chelator in duckweed systems (Baken et al., 2011). Thus, the NADH observed in this study, a kind of enzymatic antioxidant, could delay or prevent heavy metals from reaching duckweed cells by diffusion limitation or chemical reactions due to the high log K_M value. However, the traits of other three fluorescence components at various Cu^{2+} concentrations were still unclear in duckweed systems.

3.5. PCA for DOM components under different Cu^{2+} concentrations

Based on the data of the maximum fluorescence intensity from PARAFAC results, the PCA can be used to further identify and classify the behaviors of the four fluorescence component at various Cu^{2+} concentrations (Wilson et al., 2000). As shown in Fig. 4a, the eigenvalues of the two principal components (PC1 63.33%; PC2 22.67%) represented up to 86% of the observations. It was indicated that the PC1 and PC2 could reflect most of the information of the all original variable (Abdulla et al., 2013). Thus, it was decided to plot factor loadings and scores on a PC1–PC2 axes plane (Fig. 4b). As shown in Fig. 4b, the loading plot showed that the four variables exhibited a positive correlation with the PC1. And the low molecular weight (LMW) (C2: tyrosine-like) with a high value contributed to the construction of PC1, while the high molecular weight (HMW) including C1 (microbial humic-like), C3 (NADH), and C4 (humic-like) showed a small value on the axis of PC1 (Luo et al.,

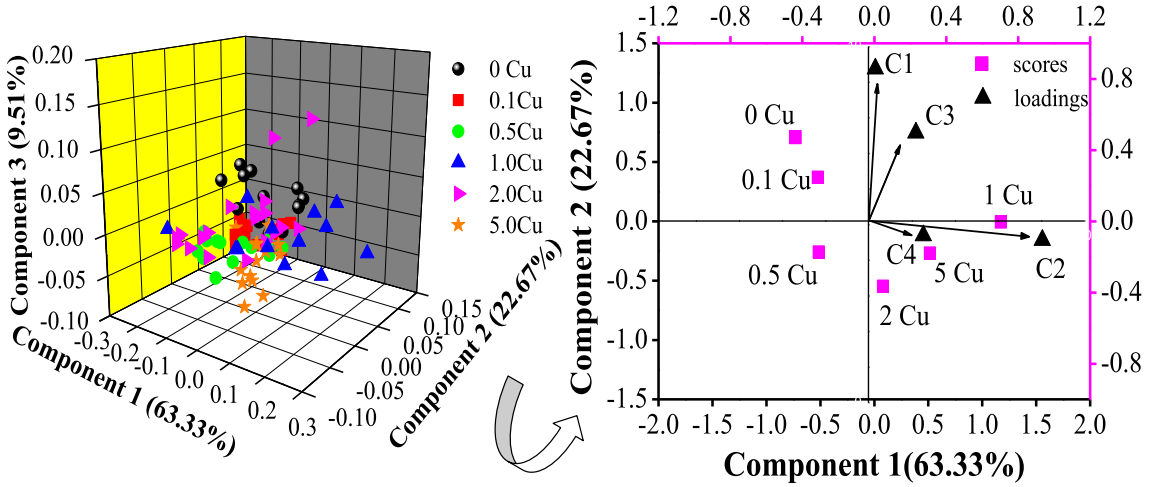

Fig. 4. PCA result based on the data of the maximum fluorescence intensity from PARAFAC result at 81samples. Left: 3-D score plot of the different samples (a); Right: 2-D biplots on component 1 and component 2 plane overlapping scores and loadings (b).

2013). It was suggested that the PC1 favored the LHW. Thus, the PC1 can be regarded as the nature of the DOM, where the LMW occupied the dominant position.

For the construction of PC2, it was found that the C1 and C3 (microbial by-products) exhibited a positive correlation with PC2, but the C2 and C4 (acidic substances) displayed a negative correlation. It indicated that the positive values of PC2 meant that the duckweed systems contain microbial by-products (eg. protein-like substance) which were in favor of the growth of aquatic plants. For the negative values of PC2, it showed that there were much acidic substances in duckweed systems, resulting in the aquatic plants adversely growing. Thus, the PC2 could be used to describe the nutrient level of duckweed systems.

Fig. 4b also showed the scores of each Cu^{2+} concentration during the period of the study. As shown in scores plot, in relation to PC1 (nature of DOM), it was found that the values of 0–0.5 mg/L Cu^{2+} were negative, while that of 1.0–5.0 mg/L Cu^{2+} were positive. It showed that few DOM released from duckweed systems at 0–0.5 mg/L of Cu^{2+}, but released in large quantities at higher Cu^{2+} concentrations. As shown in scores plot, in relation to PC1 (nature of DOM), it was found that the values of 0–0.5 mg/L Cu^{2+} were negative, while the values of 1.0–5.0 mg/L Cu^{2+} were positive. It showed that few DOM released from duckweed systems at 0–0.5 mg/L of Cu^{2+}, but released in large quantities at higher Cu^{2+} concentrations. The anti-oxidative defense system of aquatic plants played a major role in overcoming stress imposed by heavy metals. It would not function to produce antioxidants for protecting the plant cells from harm by heavy metals until the concentrations of heavy metals reached to a certain value. Thus, the release of DOM at the higher Cu^{2+} concentrations (>0.5 mg/L) indicated that DOM belonged to the anti-oxidative defense system of aquatic plants and were naturally occurring antioxidants under heavy metal stress, which was consistent with the report of Janssen and Mcneill (2014). Besides, the large value of PC1 indicated that the released DOM were mainly of low molecular weight (LMW) at 1.0 mg/L of Cu^{2+}, while the small value of PC1 indicated that they were mainly of high molecular weight (HMW) at 2.0–5.0 mg/L of Cu^{2+} in duckweed systems. In relation to PC2 (nutrient level of duckweed systems), lower Cu^{2+} concentrations (0–0.1 mg/L Cu^{2+}) were to be found in the positive part of PC2, while 0.5–5.0 mg/L Cu^{2+} were in the negative part. It was implied that the low Cu^{2+} concentrations were beneficial to the growth of duckweed through producing much protein-rich substances into the water. On the contrary, high Cu^{2+} concentrations would inhibit duckweed growth where acidic substances dominant the nutrient level of duckweed systems. This explanation was in agreement with observations in Fig. S2. Therefore, as a statistical tool, PCA can be applied to further illustrate the characteristics of DOM components and nutrient levels of duckweed systems at various Cu^{2+} concentrations.

3.6. *Effect of Cu^{2+} concentrations on the molecular characteristics of DOM*

Combining FTIR with 2D-CoS or PCMW2D would provide a clear insight into the molecular characteristics of DOM with copper ions perturbation (Abdulla et al., 2013; Lumsdon and Fraser, 2005). The 2400-800 cm^{-1} regions of 2D-FTIR-CoS were analyzed, and the results were displayed in Fig. 5 and Table 2. Fig. 5 showed the synchronous and asynchronous FTIR maps of DOM with Cu^{2+} concentration as the perturbation. The synchronous maps (Fig. 5a) exhibited seven prominent auto-peaks on the diagonal at 2334, 2217, 1912, 1560, 1162, 1104, and 887 cm^{-1}.

Considering the four fluorescence components in DOM, the cellulose and hemi-cellulose in plant, the extracellular polymeric substances (EPS) secreted by rhizosphere microorganisms, and the

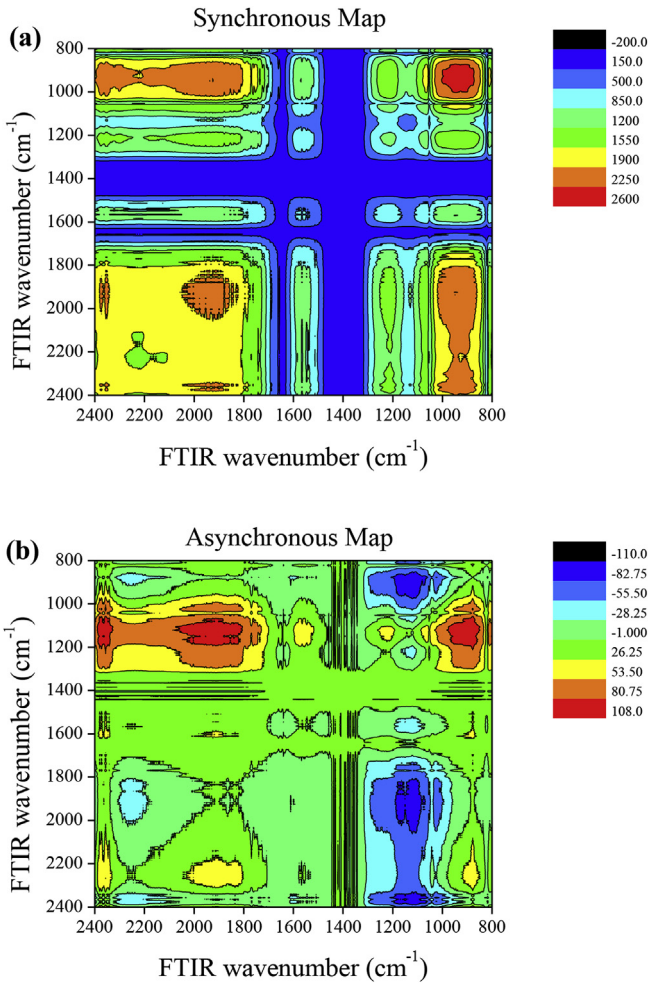

Fig. 5. Synchronous (a) and asynchronous (b) 2D correlation maps generated from the 2400-800 cm^{-1} region of the FTIR spectra of DOM released from duckweed systems with the increasing Cu^{2+} concentrations.

NO_3^- in solution, the bands at 2334 $cm^{-1}$was attributed to saturated C–H stretching of humic-like substances (Chew et al., 2013), the band at 2217 cm^{-1} was assigned to tyrosine N–H stretching vibration (Ulrici, 2004), the bands at 1912 $cm^{-1}$was generated by the N=O of deprotonated nitric acid (NO_3^-) (Xiang et al., 2015), the band at 1560 cm^{-1} correspond to the COO– symmetric stretching of tyrosine (Chen et al., 2014), the band at 1162 cm^{-1} was assigned to anti-symmetric bridge stretching of C–O–C in cellulose and hemi-cellulose (Ibrahim and Alfifi, 2010), the bands at 1104 cm^{-1} was attributed to C–O stretching of polysaccharides (Soong et al., 2014), and the band at 887 to cm^{-1} to aromatic C–H deformation in tyrosine (Chen et al., 2015b).

In addition, the change in band intensity followed the order: 887 > 1912 > 2217 > 1162 >1560 > 1104 > 2334 cm^{-1}. Meanwhile, all the cross-peaks off the diagonal exhibited positive signs in the synchronous map, indicating that these peaks exhibited the same responses of spectral intensities to copper ions perturbation. Additionally, the asynchronous spectra can help to judge the sequential order of specific events along external perturbations. The cross-peaks of every two bands were shown in Fig. 5b, and the detailed assignments of bands and signs of their cross-peaks in the asynchronous map were summarized in Table 2. In the asynchronous map, the red represents a positive sign, while the blue represents a negative sign. According to Noda's rule (Noda, 2014), the

Table 2
2D-FTIR-CoS Results on the Assignment and Sign of Each Cross-Peak in Synchronous (Φ) and Asynchronous (Ψ, in the brackets) Maps of DOM with Copper Binding.

position (cm^{-1})	possible assignment	sign						
		2334	2217	1912	1560	1162	1104	887
2334	humic-like ν_{C-H}	+	+(+)	+(0)	+(+)	+(+)	+(+)	+(0)
2217	tyrosine ν_{N-H}		+	+(−)	+(0)	+(+)	+(+)	+(−)
1912	NO_3^- $\nu_{N=O}$			+	+(0)	+(+)	+(+)	+(0)
1560	tyrosine ν_{COO^-}				+	+(+)	+(+)	+(−)
1162	cellulose ν_{C-O-C}					+	+(+)	+(−)
1104	polysaccharides ν_{C-O}						+	+(−)
887	tyrosine ν_{C-H}							+

(Signs were obtained in the upper-left corner of the maps, + positive, − negative).

sequence of bond variation with copper ions followed the order: 2334, 1912, 887 → 2217, 1536 → 1162 → 1104 cm^{-1}. Thus, as stimulated by copper ion stress, the binding order of DOM to copper ions followed the order: C—H (humic-like substances), N=O (NO_3^-), Ar—H (tyrosine) > tyrosine N—H, tyrosine COO^- > C—O—C (cellulose) > polysaccharides C—O. Clearly, according this order, the bonding of N—H and COO^- to copper ions occurred at the same time, which indirectly demonstrated that the N—H and COO^- both belonged to the functional groups of tyrosine. In brief, these observations indicated that DOM could interact with copper ions through multiple mechanisms due to its diverse functional moieties, which also exhibited the complexity and difficulty in the bonding process analysis (Chen et al., 2014; Lin et al., 2018).

As to the change of DOM conformations, the PCMW2D synchronous spectra of DOM were presented in Fig. 6. Three dominant correlation peaks at coordinates around 887 cm^{-1}/0.5 mg/L, 1912 cm^{-1}/0.5 mg/L and 2334 cm^{-1}/0.5 mg/L were observed, suggesting that the variation of DOM conformations occurred at a critical concentration of 0.5 mg/L Cu^{2+} on the pressure of Cu^{2+} concentrations. It also demonstrated that the functional groups of C—H (humic-like substances), N=O (NO_3^-), Ar—H (tyrosine) would simultaneously give the fastest binding with Cu^{2+} in the duckweed systems as stated above.

Moreover, these three functional groups were also most likely for the variation of DOM conformations with copper ions fluctuation. With respect to the conformation change of Ar—H in tyrosine, it might be induced by the unfolding of the secondary structure in tyrosine. The similar change in the protein-like substances with aromatic structure was observed by Chen et al. (2017), who demonstrated that copper ions could destroy the original hydrogen bonding network of the backbone and make the secondary structure to unfold. As for the conformation change of C—H in humic-like substances, it was possible that the spheroidal humic-like substances were surrounded by copper ions so that the molecular volume increased, and thereby the resistance to rotation and the rotation rate decreased in the solution (Lakshman et al., 1996). Therefore, humic-like substances began to exist in the form of planar expansion when exposed to a given Cu^{2+} concentration (Lakshman et al., 1996).

For the conformation change of N=O in NO_3^-, isolated NO_3^- has high symmetry with plane triangle structure, meaning that the nitrogen atom is located in the center of the regular triangle, the bond length is 1.26 Å, and the bond angle is 120 °C. However, Kameda et al. (2006) found that due to the effect of sodium ions, the NO_3^- would turn into spatial structure with 170.7° of plane degree, the bond length was 1.28 Å, and the bond angle was 119.8° via the calculation of density functional theory (DFT), but the NO_3^- was still highly symmetric (Kameda et al., 2006). Thus, it can be inferred that NO_3^- would present in similar conformational change with the copper ions perturbation. It meant conformation change of N=O in NO_3^- from plane triangle structure into spatial structure with the increase of Cu^{2+} concentrations. To make the conformation change process of DOM with copper ions more intuitive, a comprehensive picture was established based on the above conjecture at a molecular level (Fig. S14).

Therefore, the fluorescent components such as the tyrosine and humic-like substances, and the non-fluorescent group such as NO_3^- played a vital role in conformational changes of DOM with copper ions perturbation. They were more sensitive to copper ions than other functional groups in DOM released from duckweed systems.

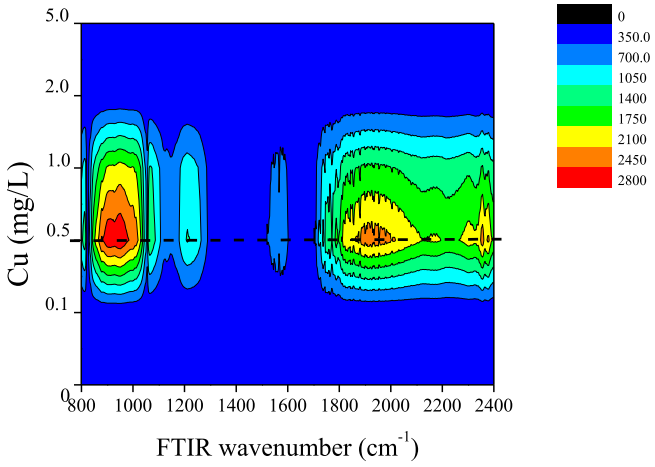

Fig. 6. PCMW2D synchronous FTIR spectra of DOM released from the duckweed systems in the region of 800–2400 cm^{-1} under the Cu^{2+} concentrations ranging from 0 to 5.0 mg/L. The dashed lines correspond to the Cu^{2+} concentration point at 0.5 mg/L.

4. Conclusions

The removal performance of ammonia nitrogen (NH_3—N) and total phosphorus (TP) could be improved at 0.1–1.0 mg/L of Cu^{2+}, while was inhibited at 2.0–5.0 mg/L of Cu^{2+} in duckweed systems for the treatment of swine wastewater. The kinetic model reached an optimal Cu^{2+} concentration of 0.96 mg/L for the removal of NH_3—N and TP in swine wastewater.

The EEM-PARAFAC analysis showed that there were four components including microbial humic-like substance, tyrosine, NADH, and humic-like substance in DOM released from the duckweed systems. Moreover, NADH exhibited high capacities of binding copper ions due to the high stability constant (log $K_M = 5.65$), which indicated that NADH was an important metal chelator in duckweed systems.

On the PCA assessment, the large value of PC1 revealed that the released DOM was mainly consisted of low molecular weight (LMW) substance at 1.0 mg/L of Cu^{2+}, while the small value of PC1 indicated that most of DOM were high molecular weight (HMW) substance at 2.0–5.0 mg/L of Cu^{2+} in duckweed systems.

The stress of Cu^{2+} on the binding order between the function groups of DOM and copper ions followed the order as: C–H, N=O, Ar–H > N–H, COO– > C–O–C > C–O according to the results of the 2D-FTIR-CoS analysis.

There existed a critical copper ion concentration of 0.5 mg/L for the variation of DOM conformations via the PCMW2D analysis, and C–H, N=O, and Ar–H were most likely responsible for the variation.

This study might provide an alternative approach for the exploration of both the interaction mechanisms of heavy metals on nutrient uptake and the role of DOM on microcosmic migration of heavy metals in duckweed systems for swine wastewater treatment.

Conflicts of interest

The authors declare that they have no known competing financial interests or personal relationships that could have appeared to influence the work reported in this paper.

Acknowledgments

This work was supported by the National Natural Science Foundation of China (Grant No.: 51478172 and 51521006), the Department of Science and Technology of Guangdong Province of China (Contract No.: 2018S0011), and the Department of Science and Technology of Hunan Province of China (Contract No.: 2017JJ2029 and 2017SK2362).

Appendix A. Supplementary data

Supplementary data to this article can be found online at https://doi.org/10.1016/j.watres.2019.04.036.

References

Abdulla, H.A.N., Minor, E.C., Dias, R.F., Hatcher, P.G., 2013. Transformations of the chemical compositions of high molecular weight DOM along a salinity transect: using two dimensional correlation spectroscopy and principal component analysis approaches. Geochem. Cosmochim. Acta 118 (10), 231–246.

Abdulla, H.A.N., Minor, E.C., Hatcher, P.G., 2010. Using two-dimensional correlations of ^{13}C NMR and FTIR to investigate changes in the chemical composition of dissolved organic matter along an estuarine transect. Environ. Sci. Technol. 44 (21), 8044–8049.

Arunachalam, R.S., Shah, H.K., Ju, L.K., 2005. Monitoring aerobic sludge digestion by online scanning fluorometry. Water Res. 39 (7), 1205–1214.

Asada, K., 1987. Production and scavenging of active oxygen in photosynthesis. Photoinhibition 228–287.

Baken, S., Degryse, F., Verheyen, L., Merckx, R., Smolders, E., 2011. Metal complexation properties of freshwater dissolved organic matter are explained by its aromaticity and by anthropogenic ligands. Environ. Sci. Technol. 45 (7), 2584–2590.

Cakmak, I., 2010. Possible roles of zinc in protecting plant cells from damage by reactive oxygen species. New Phytol. 146 (2), 185–205.

Chen, M., Xu, P., Zeng, G.M., Yang, C.P., Huang, D.L., Zhang, J.C., 2015a. Bioremediation of soils contaminated with polycyclic aromatic hydrocarbons, petroleum, pesticides, chlorophenols and heavy metals by composting: applications, microbes and future research needs. Biotechnol. Adv. 33 (6), 745–755.

Chen, W., Habibul, N., Liu, X.Y., Sheng, G.P., Yu, H.Q., 2015b. FTIR and synchronous fluorescence heterospectral two-dimensional correlation analyses on the binding characteristics of copper onto dissolved organic matter. Environ. Sci. Technol. 49 (4), 2052–2058.

Chen, W., Liu, X.Y., Yu, H.Q., 2017. Temperature-dependent conformational variation of chromophoric dissolved organic matter and its consequent interaction with phenanthrene. Environ. Pollut. 222, 23–31.

Chen, W., Qian, C., Liu, X.Y., Yu, H.Q., 2014. Two-dimensional correlation spectroscopic analysis on the interaction between humic acids and TiO2 nanoparticles. Environ. Sci. Technol. 48 (19), 11119–11126.

Chen, Y.J., He, H.J., Liu, H.Y., Li, H.R., Zeng, G.M., Xia, X., Yang, C.P., 2018. Effect of salinity on removal performance and activated sludge characteristics in sequencing batch reactors. Bioresour. Technol. 249, 890–899.

Cheng, J.J., Bergmann, B.A., Classen, J.J., Stomp, A.M., Howard, J.W., 2002. Nutrient recovery from swine lagoon water by *Spirodela punctata*. Bioresour. Technol. 81 (1), 81–85.

Cheng, J.J., Stomp, A.M., 2009. Growing duckweed to recover nutrients from wastewaters and for production of fuel ethanol and animal feed. Clean. - Soil, Air, Water 37 (1), 17–26.

Cheng, Y., He, H.J., Yang, C.P., Zeng, G.M., Li, X., Chen, H., Yu, G.L., 2016. Challenges and solutions for biofiltration of hydrophobic volatile organic compounds. Biotechnol. Adv. 34 (6), 1091–1102.

Chew, K.Y., Bakar, M.A., Bakar, N.H.H.A., 2013. Synthesis of barium nickel titanium oxide stabilized by citric acid. Model. Simul. Mater. Sc. 3 (1B), 23–27.

Chiang, P.N., Chiu, C.Y., Wang, M.K., Chen, B.T., 2011. Low-wolecular-weight organic acids exuded by millet (setaria italica (L.) beauv.) roots and their effect on the remediation of cadmium-contaminated soil. Soil Sci. 176 (1), 33–38.

Du, H.X., Harata, N., Li, F.S., 2018. Responses of riverbed sediment bacteria to heavy metals: integrated evaluation based on bacterial density, activity and community structure under well-controlled sequencing batch incubation conditions. Water Res. 130, 115–126.

EPA of China, 2002. Water and Wastewater Monitoring Analysis Method, fourth ed. Chinese Environment Science Publisher, Bejing.

He, H.J., Chen, Y.J., Li, X., Cheng, Y., Yang, C.P., Zeng, G.M., 2017. Influence of salinity on microorganisms in activated sludge processes: a review. Int. Biodeterior. Biodegrad. 119, 520–527.

Hu, H.D., Liao, K.W., Shi, Y.J., Ding, L.L., Zhang, Y., Ren, H.Q., 2018. Effect of solids retention time on effluent dissolved organic nitrogen in the activated sludge process: studies on bioavailability, fluorescent components, and molecular characteristics. Environ. Sci. Technol. 52 (6), 3449–3455.

Ibrahim, M., Alfifi, Z., 2010. Mechanism of pollution control for aquatic plant water hyacinth. Open Spectrosc. J. 4 (1), 10–15.

Janssen, E.M., Mcneill, K., 2014. Environmental photoinactivation of extracellular phosphatases and the effects of dissolved organic matter. Environ. Sci. Technol. 49 (2), 889–896.

Kameda, Y., Sugawara, K., Usuki, T., Uemura, O., 2006. Hydration structure of Na^+ in concentrated aqueous solutions. Bull. Chem. Soc. Jpn. 71 (12), 2769–2776.

Kowalczuk, P., Durako, M.J., Young, H., Kahn, A.E., Cooper, W.J., Gonsior, M., 2009. Characterization of dissolved organic matter fluorescence in the South Atlantic Bight with use of PARAFAC model: interannual variability. Mar. Chem. 113 (3–4), 182–196.

Lakshman, S., Mills, R., Feng, F., Patterson, H., Cronan, C., 1996. Use of fluorescence polarization to probe the structure and aluminum complexation of three molecular weight fractions of a soil fulvic acid. Anal. Chim. Acta 321 (1), 113–119.

Li, J., Zhou, Q., Campos, L.C., 2017. Removal of selected emerging PPCP compounds using greater duckweed (*Spirodela polyrhiza*) based lab-scale free water constructed wetland. Water Res. 126, 252–261.

Li, W.H., Sheng, G.P., Liu, X.W., Yu, H.Q., 2008. Characterizing the extracellular and intracellular fluorescent products of activated sludge in a sequencing batch reactor. Water Res. 42 (12), 3173–3181.

Li, W.H., Sheng, G.P., Lu, R., Yu, H.Q., Li, Y.Y., Harada, H., 2011. Fluorescence spectral characteristics of the supernatants from an anaerobic hydrogen-producing bioreactor. Appl. Microbiol. Biotechnol. 89 (1), 217–224.

Li, X., Yang, W.L., He, H., Wu, S.H., Zhou, Q., Yang, C.P., Zeng, G.M., Luo, L., Lou, W., 2018. Responses of microalgae *Coelastrella* sp. to stress of cupric ions in treatment of anaerobically digested swine wastewater. Bioresour. Technol. 251, 274–279.

Lin, Y., Wu, S.H., Li, X., Wu, X., Yang, C.P., Zeng, G.M., Peng, Y.R., Zhou, Q., Lu, L., 2018. Microstructure and performance of Z-scheme photocatalyst of silver phosphate modified by MWCNTs and Cr-doped SrTiO3 for malachite green degradation. Appl. Catal. B Environ. 227, 557–570.

Lumsdon, D.G., Fraser, A.R., 2005. Infrared spectroscopic evidence supporting heterogeneous site binding models for humic substances. Environ. Sci. Technol. 39 (17), 6624–6631.

Luo, K., Yang, Q., Li, X.M., Chen, H.B., Liu, X., Yang, G.J., Zeng, G.M., 2013. Novel insights into enzymatic-enhanced anaerobic digestion of waste activated sludge by three-dimensional excitation and emission matrix fluorescence spectroscopy. Chemosphere 91 (5), 579–585.

Luo, L., He, H.J., Yang, C.P., Wen, S.H., Zeng, G.M., Wu, M.J., Zhou, Z.L., Lou, W., 2016. Nutrient removal and lipid production by Coelastrella sp. in anaerobically and aerobically treated swine wastewater. Bioresour. Technol. 216, 135–141.

Matthias, P., Timr, M., Maltaf, A., Mike, D., David, B., Joshua, M.L., 2007. Concentrations and fluxes of dissolved organic carbon in an age-sequence of white pine forests in Southern Ontario, Canada. Biogeochemistry 86 (1), 1–17.

Morita, S., Shinzawa, H., Noda, I., Ozaki, Y., 2006. Perturbation-correlation moving-window two-dimensional correlation spectroscopy. Appl. Spectrosc. 60 (4), 398–406.

Murphy, K.R., Adam, H., Sachin, S., Henderson, R.K., Andy, B., Richard, S., Khan, S.J., 2011. Organic matter fluorescence in municipal water recycling schemes: toward a unified PARAFAC model. Environ. Sci. Technol. 45 (7), 2909–2916.

Noda, I., 2014. Frontiers of two-dimensional correlation spectroscopy. Part 1. new concepts and noteworthy developments. J. Mol. Struct. 1069 (1), 3–22.

Obermeier, M., Schroder, C.A., Helmreich, B., Schroder, P., 2015. The enzymatic and antioxidative stress response of *Lemna minor* to copper and a chloroacetamide herbicide. Environ. Sci. Pollut. Res. Int. 22 (23), 18495–18507.

Ohno, T., Amirbahman, A., Bro, R., 2008. Parallel factor analysis of excitation-emission matrix fluorescence spectra of water soluble soil organic matter as basis for the determination of conditional metal binding parameters. Environ. Sci. Technol. 42 (1), 186–192.

Pant, D., Adholeya, A., 2009. Nitrogen removal from biomethanated spentwash using hydroponic treatment followed by fungal decolorization. Environ. Eng.

Sci. 26 (3), 559–565.
Peng, S., Li, H.J., Song, D., Lin, X.G., Wang, Y.M., 2018. Influence of zeolite and superphosphate as additives on antibiotic resistance genes and bacterial communities during factory-scale chicken manure composting. Bioresour. Technol. 263, 393–401.
Poulin, B.A., Ryan, J.N., Aiken, G.R., 2014. Effects of iron on optical properties of dissolved organic matter. Environ. Sci. Technol. 48 (17), 10098–10106.
Rengel, Z., 2002. Genetic control of root exudation. Plant Soil 245 (1), 59–70.
Rosario-Ortiz, F.L., Snyder, S.A., Suffet, I.H., 2007. Characterization of dissolved organic matter in drinking water sources impacted by multiple tributaries. Water Res. 41 (18), 4115–4128.
Senesi, N., 1990. Molecular and quantitative aspects of the chemistry of fulvic acid and its interactions with metal ions and organic chemicals. Part II. The fluorescence spectroscopy approach. Anal. Chim. Acta 232 (3), 51–75.
Senga, Y., Yabe, S., Nakamura, T., Kagami, M., 2018. Influence of parasitic chytrids on the quantity and quality of algal dissolved organic matter (AOM). Water Res. 145, 346–353.
Soong, J.L., Calderon, F.J., Betzen, J., Cotrufo, M.F., 2014. Quantification and FTIR characterization of dissolved organic carbon and total dissolved nitrogen leached from litter: a comparison of methods across litter types. Plant Soil 385 (1–2), 125–137.
Sun, J.X., Yuan, X.Z., Shi, X.S., Chu, C.F., Guo, R.B., Kong, H.N., 2011. Fermentation of *Chlorella* sp. for anaerobic bio-hydrogen production: influences of inoculum-substrate ratio, volatile fatty acids and NADH. Bioresour. Technol. 102 (22), 10480–10485.
Tandon, S.A., Kumar, R., Yadav, S.A., 2013. Pytoremediation of fluoroquinolone group of antibiotics from waste water. Nat. Sci. 5 (12A), 21–27.
Teixeira, A.P., Duarte, T.M., Oliveira, R., Carrondo, M.J.T., Alves, P.M., 2011. High-throughput analysis of animal cell cultures using two-dimensional fluorometry. J. Biotechnol. 151 (3), 255–260.
Ulrici, W., 2004. Hydrogen-impurity complexes in III-V semiconductors. Rep. Prog. Phys. 67 (12), 2233–2286.
Vermaat, J.E., Hanif, M.K., 1998. Performance of common duckweed species (*Lemnaceae*) and the waterfern Azolla filiculoides on different types of waste water. Water Res. 32 (9), 2569–2576.
Wang, J.L., Chen, C., 2009. Biosorbents for heavy metals removal and their future. Biotechnol. Adv. 27 (2), 195–226.
Wei, L.L., Zhao, Q.L., Xue, S., Jia, T., Tang, F., You, P.Y., 2009. Behavior and characteristics of DOM during a laboratory-scale horizontal subsurface flow wetland treatment: effect of DOM derived from leaves and roots. Ecol. Eng. 35 (10), 1405–1414.
Wen, S., Liu, H.Y., He, H.J., Luo, L., Li, X., Zeng, G.M., Zhou, Z.L., Lou, W., Yang, C.P., 2016. Treatment of anaerobically digested swine wastewater by *Rhodobacter blasticus* and *Rhodobacter capsulatus*. Bioresour. Technol. 222, 33–38.
Wilson, R.H., Smith, A.C., Kacurakova, M., Saunders, P.K., Wellner, N., Waldron, K.W., 2000. The mechanical properties and molecular dynamics of plant cell wall polysaccharides studied by Fourier-transform infrared spectroscopy. Plant Physiol. 124 (1), 397–405.
Wu, J., Zhang, H., Yao, Q.S., Shao, L.M., He, P.J., 2012. Toward understanding the role of individual fluorescent components in DOM-metal binding. J. Hazard Mater. 215–216 (4), 294–301.
Wu, S.H., He, H.J., Li, X., Yang, C.P., Zeng, G.M., Wu, B., He, S.Y., Lu, L., 2018. Insights into atrazine degradation by persulfate activation using composite of nanoscale zero-valent iron and graphene: performances and mechanisms. Chem. Eng. J. 341, 126–136.
Wu, S.H., Shen, Z.Q., Yang, C.P., Zhou, Y.X., Li, X., Zeng, G.M., Ai, S.J., He, H.J., 2017. Effects of C/N ratio and bulking agent on speciation of Zn and Cu and enzymatic activity during pig manure composting. Int. Biodeterior. Biodegrad. 119, 429–436.
Xiang, H.J., An, L., Tang, W.W., Yang, S.P., Liu, J.G., 2015. Photo-controlled targeted intracellular delivery of both nitric oxide and singlet oxygen using a fluorescence-trackable ruthenium nitrosyl functional nanoplatform. Chem. Commun. 51 (13), 2555–2558.
Xu, H.C., Yu, G.H., Yang, L.Y., Jiang, H.L., 2013. Combination of two-dimensional correlation spectroscopy and parallel factor analysis to characterize the binding of heavy metals with DOM in lake sediments. J. Hazard Mater. 263 Pt 2, 412–421.
Xu, J.L., Shen, G.X., 2011. Growing duckweed in swine wastewater for nutrient recovery and biomass production. Bioresour. Technol. 102 (2), 848–853.
Yamashita, Y., Jaffe, R., 2008. Characterizing the interactions between trace metals and dissolved organic matter using excitation-emission matrix and parallel factor analysis. Environ. Sci. Technol. 42 (19), 7374–7379.
Yang, C.P., Qian, H., Li, X., Cheng, Y., He, H.J., Zeng, G.M., Xi, J.Y., 2018. Simultaneous removal of multicomponent VOCs in biofilters. Trends Biotechnol. 36 (7), 673–685.
Zhang, K., Chen, Y.P., Zhang, T.T., Zhao, Y., Shen, Y., Huang, L., Gao, X., Guo, J.S., 2014. The logistic growth of duckweed (*Lemna minor*) and kinetics of ammonium uptake. Environ. Technol. 35 (5–8), 562–567.
Zhou, Q., Lin, Y., Li, X., Yang, C.P., Han, Z.F., Zeng, G.M., Lu, L., He, S.Y., 2018. Effect of zinc ions on nutrient removal and growth of Lemna aequinoctialis from anaerobically digested swine wastewater. Bioresour. Technol. 249, 457–463.
Zhu, G.C., Bian, Y.N., Hursthouse, A.S., Wan, P., Szymanska, K., Ma, J., Wang, X.F., Zhao, Z.L., 2017. Application of 3-D fluorescence: characterization of Natural organic matter in natural water and water purification systems. J. Fluoresc. 27 (9), 1–26.
Zhu, G.C., Yin, J., Zhang, P., Wang, X.F., Fan, G.D., Hua, B., Ren, B.Z., Zheng, H.L., Deng, B.L., 2014. DOM removal by flocculation process: fluorescence excitation–emission matrix spectroscopy (EEMs) characterization. Desalination 346, 38–45.